Journal of Applied Microbiology ISSN 1364-5072

ORIGINAL ARTICLE

Localization of norovirus and poliovirus in Pacific oysters

C. Mcleod[1], B. Hay[2], C. Grant[2], G. Greening[3] and D. Day[1]

1 School of Biological Sciences, Victoria University of Wellington, Wellington, New Zealand
2 AquaBio Consultants Ltd, Auckland, New Zealand
3 Institute of Environmental Science and Research Limited, Porirua, New Zealand

Keywords
immunohistochemistry, localization, norovirus, Pacific oysters, polymerase chain reaction, poliovirus.

Correspondence
Darren Day, School of Biological Sciences, Victoria University of Wellington, PO Box 600, Wellington, New Zealand.
E-mail: darren.day@vuw.ac.nz

Present address
Catherine McLeod, South Australian Research and Development Institute, Glenside, Adelaide, South Australia.

2008/0937: received 2 June 2008, revised 18 September 2008 and accepted 24 September 2008

doi:10.1111/j.1365-2672.2008.04091.x

Abstract

Aims: To examine the uptake and tissue distribution of norovirus (NoV) and poliovirus (PV) experimentally bioaccumulated in feeding Pacific oysters (*Crassostrea gigas*).

Methods and Results: Pacific oysters were allowed to bioaccumulated either PV or NoV under tidally synchronized feeding conditions in laboratory tanks. Oysters were then either fixed and paraffin wax embedded prior to localizing virus within tissues by immunohistochemistry (IHC), or they were dissected into digestive tract (stomach, intestine and digestive diverticula), gill and labial palp tissues, and the viral load determined by quantitative RT-PCR. Both PV and NoV immunoreactivities were predominantly found in the lumen and within cells of the digestive tract tissues; however, PV was also found within cells of nondigestive tract tissues, and in the gills and labial palp. Quantitative RT-PCR of tissue extracts corroborate the immunohistochemical data in that the major site for virus localization is the gut, but significant amounts of viral RNA were identified in the gills and labial palp.

Conclusions: The human enteric viruses, PV and NoV, are readily bioaccumulated by feeding Pacific oysters and that some of the virus is internalized within cells of both digestive and nondigestive tissues.

Significance and Impact of the Study: Oysters that have been virally contaminated even after depuration (cleaning) in uncontaminated seawater could pose a human health risk if consumed.

Introduction

Pacific oysters naturally inhabit intertidal areas that can be episodically contaminated with human faeces or sewage. Oysters acquire their food by filter feeding using cilia on the gill surface to produce water currents to capture food particles in mucus on the gills. The gills transport food particles via a string of mucus forward to the labial palps, where particles are either guided to the mouth for ingestion or dropped into the mantle cavity and rejected as pseudofaeces (Ward *et al.* 1997, 1998). It has been suggested that both particle size and other properties such as charge and nutritional value may influence food selection by oysters (Shumway *et al.* 1985; Ward *et al.* 1997).

A variety of human enteric viruses have been directly detected in shellfish, or have been linked to human shellfish consumption through epidemiological studies (Lees 2000). Norovirus (NoV) and hepatitis A are predominant causes of illness linked to shellfish consumption in many countries (Jones and Graham 1995; Greening *et al.* 2001a; Simmons *et al.* 2001; Koopmans *et al.* 2002; Butt *et al.* 2004), these and other viruses such as poliovirus (PV), have been detected in naturally grown bivalve shellfish (Bendinelli and Ruschi 1969; Lewis *et al.* 1986; Green and Lewis 1999; Lees 2000; Chironna *et al.* 2002; Formiga-Cruz *et al.* 2002; Lowther *et al.* 2008). PV and NoV are structurally similar in their size, shape and buoyant density, and also in that they both lack lipid envelopes and have single stranded RNA genomes of approximately 7500 nucleotides. In spite of these similarities, the viruses may differ considerably as their capsids are made up of different types of proteins, and their host cell receptors

are thought to be different (Greenberg *et al.* 1981; Kapikian *et al.* 1996; Ashida and Hamada 1997; Feigelstock *et al.* 1998; Hollinger and Emerson 2001; Racaniello 2001, 2006; Büchen-Osmond 2004).

The digestive tract is the major site for accumulation of PV and NoV (Di Girolamo *et al.* 1975; Schwab *et al.* 1998), and *in situ* localization studies have established that some viruses are taken into digestive tract cells of oysters. A recent study suggests that NoV is localized within phagocytes and in the lumen of digestive diverticula tubules of Pacific oysters (Le Guyader *et al.* 2006), while other research demonstrated the presence of cricket paralysis virus (an insect picornavirus) in cells of the digestive diverticula and intestine (mid-gut) epithelium (Hay and Scotti 1986). Similar studies have identified ingested hepatitis A virus (HAV) in basal cells of the stomach epithelium in *Crassostrea virginica* (Romalde *et al.* 1994). The cell types responsible for virus uptake in the Pacific oyster digestive tract, and the mode of uptake, still require elucidation. *In situ* data relating to the distribution of viruses in tissues outside the oyster digestive tract such as the gills and labial palps are also limited.

The aim of this study was to determine the tissue and cellular distribution of PV and NoV within Pacific oyster tissues. We have used the Sabin strain of PV as a surrogate model for enteroviral infection as the virus is less hazardous to work with, and can be readily cultured and detected by PCR and immunohistochemistry (IHC). In this paper, we report the presence of PV and NoV within cells and the lumen of the digestive tract tissues, and within some cells of nondigestive tract tissues. While viruses within the oyster digestive tract lumen are likely to be depurated rapidly when oysters are placed in clean water, elimination or inactivation of virus that has been taken into cells may be much slower. These findings are of significance when considering the depuration of human enteric viruses from oysters intended for human consumption.

Materials and methods

Viruses

Poliovirus (Sabin vaccine strain) stock inoculum was prepared from infected buffalo green monkey kidney cells, as described previously (Greening *et al.* 2001b). A stock inoculum of NoV Farmington Hills-like strain (genotype GII/4) (Zheng *et al.* 2006) was prepared from NoV-positive faecal specimens (Greening *et al.* 2001a; Hewitt and Greening 2004). In brief, faeces were resuspended by vortexing in 10 volumes of viral transport medium (a 10% w/v faeces solution). The virus transport medium (pH 7·3) consisted of 500 ml minimum essential medium with Earles salts and L-glutamine (Gibco, Invitrogen Corp., Auckland, NZL), 33·3 ml 7·5% BSA (Sigma, St Louis, USA), 12·5 ml HEPES (Gibco, Invitrogen), 125 000 units of Mycostatin (Sigma), 100 units of penicillin G sulfate and 100 μg ml^{-1} streptomycin sulfate (Gibco, Invitrogen). The suspension was then clarified in chloroform (1 volume) and centrifuged at 12 000 ***g*** for 10 min at 4°C. The supernatant was then transferred to a fresh sterile vial and stored at 4°C until used.

Laboratory bioaccumulation

All Pacific oysters were harvested from the Mahurangi Harbour in New Zealand, an area that is classified by the New Zealand Food Safety Authority as 'approved' for commercial shellfish harvesting. The oysters were scrubbed to remove fouling organisms prior to experimentation. The temperature of the seawater during the experiments was ambient (approx. 20°C) and the salinity 30 ppt. Total ammonia levels in the tanks were monitored throughout the experiments (Tetra Test Total Ammonia Kit; Tetra, DEU, Germany). To mimic the tidal cycle and maintain the associated oyster digestive rhythms throughout the experiments, once in each 12-h period the oysters were removed from the tanks for 3 h, and re-submerged in synchrony with the tidal cycle of the Mahurangi Harbour. Prior to the experiments, oysters were acclimatized to experimental conditions for at least 48 h.

Each tank contained 80 l of aerated seawater and 60 oysters were positioned on wire mesh trays in each of the two tanks used for this experiment. Oysters were held in seawater containing either PV [2×10^8 PCR amplifiable units (PAU) per oyster; 37 500 PAU ml^{-1}] or NoV ($4{\cdot}2 \times 10^5$ PAU per oyster; 80 PAU ml^{-1}) for 48 h. The oysters were fed a quarter of the total stock inocula with each 'tidal' change of seawater (three changes in 48 h). The amount of NoV in the virus inoculum was lower than that used for PV because NoV cannot be propagated in conventional cell culture, and low titres of NoV were present in the human faecal samples from which the inoculum was prepared. For both PV and NoV experiments, a group of eight oysters that were not exposed to virus served as controls.

Oyster sample preparation

Preliminary experiments showed that the adductor muscle and mantle tissue contained minimal amount of virus, therefore, to reduce the number of samples requiring analysis, only the digestive tract (stomach, intestine and digestive diverticula), gill and labial palp tissues were analysed (Fig. 1). Immediately following bioaccumulation, oysters were dissected into the three tissue types and the

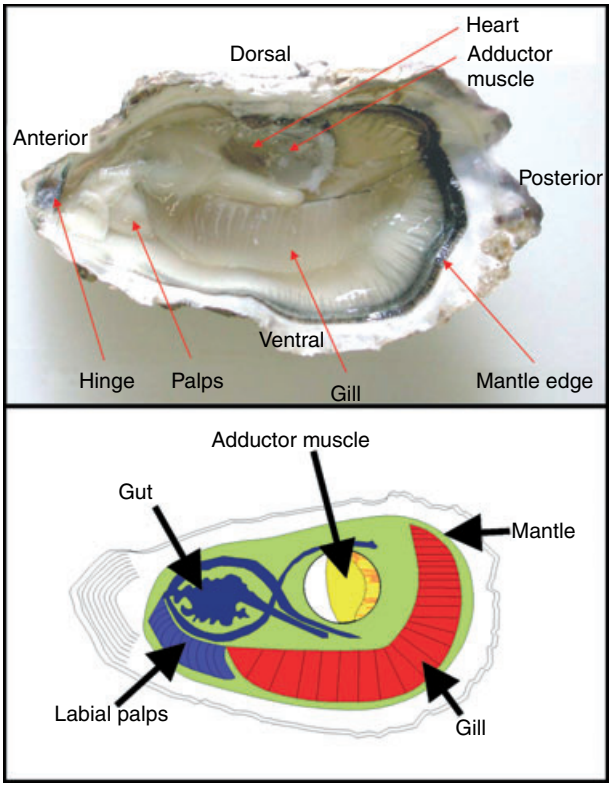

Figure 1 The anatomy of an oyster. The top panel shows a photograph of the main anatomical structures of a Pacific oyster (photograph kindly supplied by Andrew Bell, Ministry of Agriculture and Forestry, New Zealand), and the bottom panel a schematic representation indicating the structure analysed in this study.

gonad was dissected from the digestive tract samples and discarded. Because oyster glycogen is a known inhibitor of RT-PCR (Atmar *et al.* 1993), the gonad was not included in the tissues analysed in this study due to difficulty in accurately quantifying virus RNA in this glycogen-rich tissue. Dissected tissues from two individual oysters were pooled to form one sample, and four such samples were taken at the end of the 48 h bioaccumulation period from each experimental group and analysed for NoV, or PV. All dissected tissue was stored at −80°C until the RNA was extracted and analysed by real-time RT-PCR (approx. 1 month period). Several whole oysters containing PV and NoV were snap-frozen using dry ice and stored at −80°C until IHC analysis (approx. 1 month period).

RNA isolation

All tissues were finely chopped using a scalpel and homogenized in a stomacher (Stomacher Lab-Blend 80, Seward Laboratory, St Edwards, UK) for 2 min. The homogenate (30 mg) was resuspended in 60 μl of phosphate buffered saline (PBS) (pH 7·3, 160 mmol l^{-1} NaCl, 3 mmol l^{-1} KCl, 1 mmol l^{-1} KH_2PO_4, 8 mmol l^{-1} Na_2HPO_4) (Oxoid, Basingstoke, UK) and mixed thoroughly by vortexing for 2 min. The homogenate was sonicated (model FX10; Unisonics Pty, Ltd, Sydney, Australia) at room temperature for 3 min, then centrifuged at 2000 ***g*** for 3 min and the supernatant collected for analysis. RNA was extracted from oyster homogenate (30 mg) by extraction with 750 μl of Trizol (Invitrogen, Life Technologies, Auckland, NZL). The aqueous phase containing RNA was recovered from the Trizol extract by the addition of chloroform (150 μl) and centrifugation at 10 000 ***g*** for 5 min. The aqueous phase was removed and 0·5 volumes of 100% ethanol (Sigma-Aldrich NZ Ltd, Auckland, NZL) added and the solution applied to a High Pure RNA Tissue Kit column (Roche Molecular Biochemicals Ltd, Mannheim, DEU, Germany). The bound RNA was washed according to the manufacturer's instructions, then eluted in 50 μl of nuclease-free water and stored at −70°C until used. Experiments in which known quantities of PV were added to oyster matrix indicated that recovery of greater than 90% of the added virus was readily achievable.

Real-time PCR analysis

To prevent contamination from previously amplified material, all PCR reactions were set up in a separate purpose-built room, and dedicated equipment, barrier pipette tips and nuclease-free reagents were used. One-step RT-PCR amplification was performed using Platinum® Quantitative RT-PCR Thermoscipt™ One-Step System (Invitrogen Corp., CA, USA) on a Rotor-Gene 3000 real-time cycler (Corbett Life Science, Sydney, Australia). Primers used are given in Table 1. The PV primers and probes have been previously described (Donaldson *et al.* 2002). GII/4 NoV real-time RT-PCR primers were designed (Primer Express™ ver. 1·5, Applied Biosystems Ltd.) and are specific for the virus RNA polymerase. Reactions (25 μl) contained 2·5 μl of RNA template, 20 U of RNase Inhibitor (RNaseOUT, Invitrogen), 0·5 μl of reverse transcriptase-*Taq* polymerase enzyme mix (Invitrogen), forward and reverse primers (0·6 μmol l^{-1} PV, 0·4 μmol l^{-1} NoV), and Taqman probe (0·25 μmol l^{-1} PV and 0·2 μmol l^{-1} NoV) appropriately diluted in the supplied amplification buffer (Invitrogen).

Following an initial 30-min reverse transcription step at 60°C, and a denaturation step at 95°C for 5 min, amplification was achieved with a thermal cycle consisting of 40 cycles of denaturation at 95°C for 20 s and annealing/extension at 60°C (PV) or 59°C (NoV) for 60 s. Data were analysed using the Rotor-Gene™ software to calculate cycle threshold (Ct) values. Data were transformed to

Table 1 Poliovirus (PV) and norovirus (NoV) primer and probe sequences

Primer or Probe	Sequence (5′ to 3′)	PCR product size	Genome region amplified
PV-for	GGC CCC TGA ATG CGG CTA AT	190 bp	5′ noncoding region; [bases 449 to 639]
PV-rev	ACC GGA TGG CCA ATC		
PV-probe	6-FAM d(CGG ACA CCC AAA GTA GTC GGT TCC G) BHQ-1		
NoV-for	AGT TGA TGT CCT TAC TGG GAG AGG	72 bp	Nonstructural poly-protein (polymerase gene); [bases 4886 to 4958]
NoV-rev	TGA CTA ACT TGC TGA TTT TGC TGT AGA		
NoV-probe	6-FAM d(CGC ACT CCA CGG CCC AGC A) BHQ-1		

BHQ-1 = Black hole quencher; 6-FAM = 5′-Fluorescein-CE Phosphoramidite; for = forward primer; rev = reverse primer.
The PV primers and probes have been previously described by Donaldson *et al.* (2002).

real-time PAU per milligram of oyster tissue (PAU mg^{-1}) using external standard curves generated from log dilutions (10^0–10^8) of NoV and PV stock preparations (Wong and Medrano 2005). All samples were assayed at least in duplicate and the mean number of PAU mg^{-1} determined.

Immunohistochemistry

Oyster tissue fixation and sectioning was carried out essentially as previously described (Howard and Smith 1983). Frozen oysters (−80°C) were cut coronally into 0·5-cm thick blocks and were fixed for 24 h in Davidson's solution (Howard and Smith 1983) and then paraffin wax (Sigma-Aldrich NZ Ltd) embedded. Tissue sections (7 μm) were cut on a microtome and mounted on Superfrost-Plus slides (BDH Laboratory Supplies, Poole, UK). Sections for staining were dewaxed in xylene (Sigma-Aldrich NZ Ltd) and re-hydrated through an ethanol (Sigma-Aldrich NZ Ltd) series. Antigen retrieval was achieved by heating slides in boiling 10 mmol l^{-1} sodium citrate (Sigma-Aldrich NZ Ltd) buffer pH 6·0 containing 0·05% Tween 20 (BDH Chemicals Ltd., Poole, UK) for 20 min and then allowing the solution to cool for a further 20 min. Slides were washed in PBS (Oxoid) and autofluorescence quenched by washing in 0·2% $NaBH_4$ (Sigma-Aldrich NZ Ltd) (3 × 10 min washes) followed by rinsing in PBS. Slides were then washed in 0·5% Triton X-100 (Sigma-Aldrich NZ Ltd) for 30 min, rinsed in PBS, and then blocked in PBS containing 6% w/v skimmed dried milk (Anchor, NZ Ltd) and 0·05% w/v saponin (Sigma-Aldrich NZ Ltd) for 90 min. For slides stained with diaminobenzidene (DAB) (Sigma) the 0·2% $NaBH_4$ treatment step was replaced with a 30-min incubation in 3% H_20_2 (Sigma-Aldrich NZ Ltd) in PBS.

Poliovirus immunoreactivity (IR) was detected with an undiluted mouse anti-PV primary antibody (Chemicon International, Temecula, CA, USA). Staining for the mouse anti-PV primary antibody was detected with an antimouse digoxigenin (DIG) conjugate (Roche, Penzberg, DEU, Germany), followed by an anti-DIG rhodamine conjugate (Roche). In some experiments, PV IR was detected with an anti-mouse AlexaFluor 488 conjugate (Molecular Probes Inc., Eugene, OR, USA).

NoV IR was detected with an undiluted rabbit anti-NoV GII primary antibody sourced from an ELISA kit (DAKO Cytomation IDEIA™, Cambs, UK). The anti-NoV primary antibody was detected with an ovine anti-rabbit DIG conjugate (Chemicon International), followed by an anti-goat AlexaFluor 488 conjugate (Molecular Probes Inc.). In some experiments, NoV IR was detected with an anti-DIG peroxidase conjugate (Roche) and was visualized by DAB (Sigma) staining (Kivell *et al.* 2004).

Primary antibodies were applied to the sections for 12 h at 4°C and slides were washed with PBS containing 0·1% Tween 20 (BDH Chemicals Ltd, Poole, UK) (eight times, 5 min each) after antibody incubation. Slides were counterstained with 10 ng ml^{-1} 4′,6-diamino-2-phenylindole (DAPI) (Molecular Probes Inc.), or in some cases with 1 μg ml^{-1} propidium iodide (Molecular Probes Inc.) prior to mounting in Antifade (Vectorshield, Burlingame, CA, USA). DAB-stained sections were mounted in DePX (BDH Laboratory Supplies, Poole, UK).

Image analysis

Slides were viewed with an Olympus AX70 compound microscope (Olympus, Tokyo, JPN) fitted with narrow band filters specific for DAPI, fluorescein and propridium iodide. The images were captured using an Olympus DP 70 digital camera and overlaid to produce dual colour images using Adobe Photoshop CS software. Some slides were viewed and photographed with a Leica TCS 40 confocal laser-scanning microscope fitted with a krypton/argon laser.

Data analysis

To identify the statistical significance, single factor ANOVA using Microsoft Excel (Microsoft® Excel 2004 for Mac®

Version 11.1, Microsoft Corporation, USA) was used. Results with *P*-values of <0·05 were considered significant.

Results

Quality control

Oysters were observed to open and close in response to submersion in seawater and removal from the tanks, and the seawater was clear within 30 min of the oysters being submerged. Total ammonia levels in the oyster tanks were found to be between 0 and 1·5 mg l^{-1} throughout the experiments, and no mortality or spawning was observed. Faeces and pseudofaeces production were observed in the tanks during the virus bioaccumulation period. Together, these observations indicate that the oysters were actively feeding and behaving normally.

The real-time RT-PCR assays were linear over a 10 000-fold range, with Ct values for the external RNA standards ranging between 12·5 and 35 cycles and correlation coefficients >0·98 being consistently achieved in each experiment. PV samples that had Ct values below 34, and NoV samples with Ct values below 35, were considered positive. PCR product was never observed in control amplifications lacking template. The limit of detection for the real-time PCR assays in shellfish was 670 PAU g^{-1} oyster tissue.

To test the reproducibility of the extraction and real-time RT-PCR method five samples of the same PV infected oyster digestive tract were individually extracted and assayed by real-time RT-PCR in triplicate. The variation between replicate extractions was 7·45% (coefficient of variation) indicating that the method was reproducible. RNA extraction and real-time RT-PCR analyses of the control oysters were undertaken and confirmed that none of the oysters used in our experiments were initially contaminated with PV or NoV.

Controls used for IHC included staining of uncontaminated oyster sections and staining of sections in which the primary antibody was omitted. No staining above background autofluorescence was observed with these negative control samples.

Localization of PV and NoV RNA by real-time RT-PCR

Following 48 h of bioaccumulation of PV and NoV, virus RNA was localized predominantly in the oyster digestive tract, with lower amounts of RNA present in the gill and labial palp tissues as expected (Table 2). The levels of NoV RNA found in the gill and labial palp tissues were significantly lower than that found in the digestive tract ($P = 0·0003$); however, the amount of PV RNA in the gill and labial palp tissues was not significantly different from that detected in the digestive tract tissue ($P = 0·069$).

Table 2 The mean PCR amplifiable units per g tissue (PAU g^{-1}) of poliovirus (PV) and norovirus (NoV) in digestive tract, gill and labial palp tissues of Pacific oysters that had bioaccumulated virus over 48 h

Virus	Tissue PAU g^{-1}	Tissue ± SEM
NoV	Gut	27 460 ± 5810
NoV	Gill	220 ± 90*
NoV	Labial palp	130 ± 70*
NoV	Seawater	80†
PV	Gut	117 520 ± 59 270
PV	Gill	8 230 ± 680
PV	Labial palp	830 ± 440
PV	Seawater	37 500†

PAU = PCR amplifiable unit; SEM = standard error of the mean.
*The limit of detection of the real-time PCR assay was 670 PAU g^{-1} tissue. Some results are reported as numbers lower than the limit of detection, but this arises from averaging data from replicate samples.
†Seawater concentrations are the PAU seeded into each tank per ml seawater (PAU ml^{-1}).

Localization of PV and NoV protein by IHC

Stomach

The majority of the PV and NoV IR is localized to the nonciliated (Fig. 2) and ciliated (Fig. 3) epithelium of the oyster stomach. Figure 2A shows a low magnification view of the stomach in which the stomach lumen and basement membrane (BM) sides of the epithelial cells can be readily distinguished. Panel B shows a microscope enlargement of the boxed region in Panel A. The majority of the PV IR is located between epithelial cells in the region adjacent to the BM, but PV IR is also present in vesicle-type structures on the lumen side of the epithelium (Panel B, white arrows). Panel C shows the granular nature of the PV IR located between the epithelial cells near the BM (Panel C, white arrowheads). Figure 2D shows the location of NoV IR (green) in a similar region of stomach to that presented in Panel C. NoV IR is also observed between stomach epithelial cells adjacent to the BM (white arrow) as for PV. Figure 3A shows PV immunofluorescence (red) counterstained with DAPI (blue) within epithelial cells in the ciliated portion of the stomach. Panels B and D show digitally enlarged regions from Panel A in which PV IR can be seen within the cytoplasm of a small round cell (Panel B, white arrow), and within the cytoplasm of an elongated columnar cell (Panel D, white arrow). Panel C shows the same section presented in Panel A stained with Haemalun and Eosin. Black arrows indicate the cells that show PV IR identified in Panels B and D.

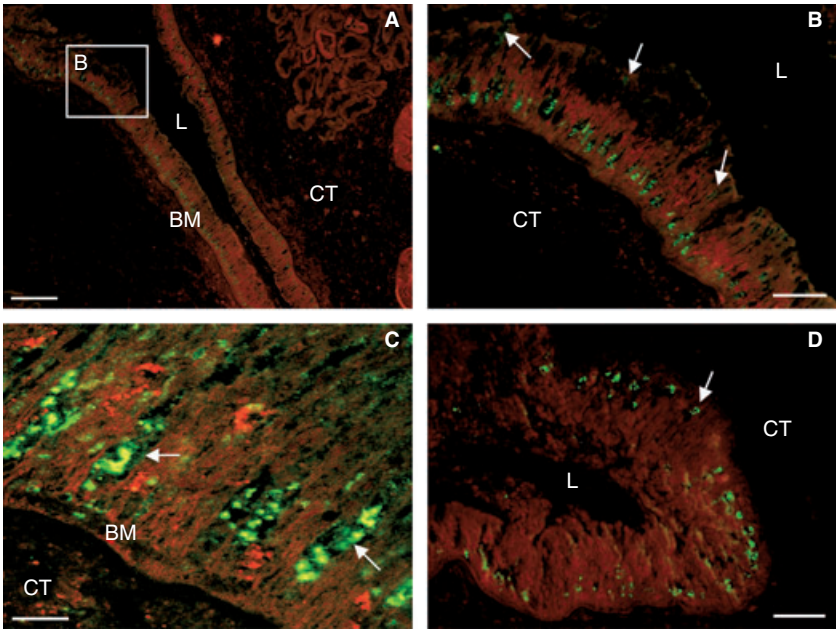

Figure 2 Localization of PV and NoV IR in stomach epithelial tissue. Panels A, B and C show staining for PV IR (green) and Panel D NoV IR (green). Cell nuclei and cytoplasm are counterstained with propridium iodide (red). Panel A shows a low magnification view of the stomach epithelium. Panel B shows an enlarged region of Panel A in which PV IR is visible between epithelial cells adjacent to the basement membrane (triangles). PV IR is also present in vesicle on the lumen side of the epithelial layer (arrows). Panel C shows an enlarged portion of stomach epithelium, in which staining of PV IR granules can be clearly seen between epithelial cells (arrows). Panel D shows NoV IR in the stomach epithelium (arrow). The staining patterns for NoV and PV are similar (compare Panels B and D). CT = connective tissue; BM = basement membrane of stomach epithelium; L = lumen. Panel A scale bar = 200 μm; Panels B and D scale bars = 20 μm; Panel C scale bar = 5 μm.

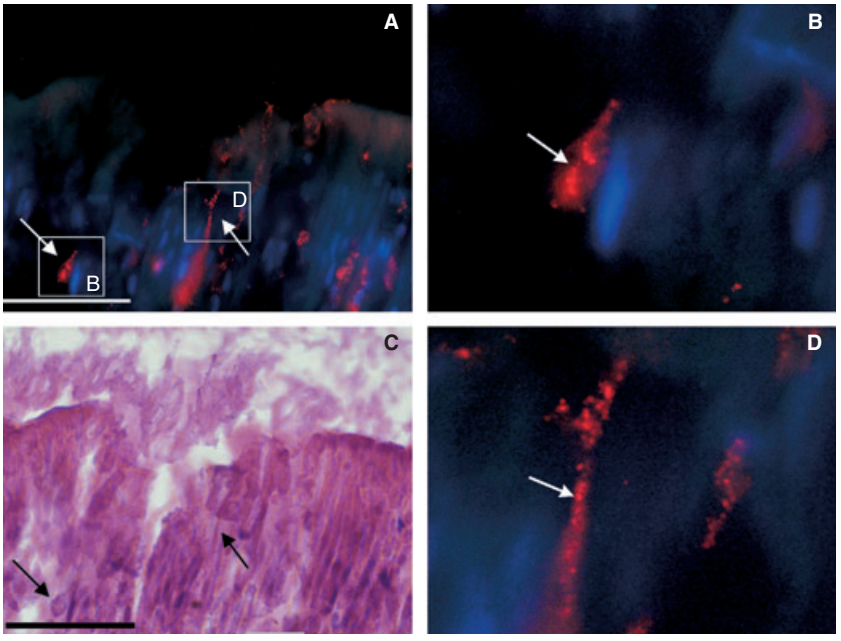

Figure 3 Localization of PV IR in the ciliated stomach epithelium. PV IR (red) was visualized with a rhodamine conjugated secondary antibody and nuclei counterstained with DAPI (blue) (Panels A, B and D). Arrows on Panel A indicate PV IR in the cytoplasm of epithelial cells. Panel C shows the same slide counterstained with Haemalun and Eosin. Black arrows indicate the highlighted cells in Panel A that are shown in higher magnification in Panels B and D. Panel B and D shows an enlarged region of Panel A, in which PV IR is located in the cytoplasm of a small round cell (Panel B) and within a long narrow cell within the stomach epithelium. Scale bars 20 μm.

Intestine

Figure 4A shows a low power view of the midgut (intestine) counterstained with propridium iodide (red). Panel B shows an enlargement of the boxed region of Panel A in which PV IR (green) is readily visualized, particularly near the typhlosole groove (TG) among food particles and mucus. Panels C and D show NoV IR (green) in similar regions of intestine to that presented in Panels A and

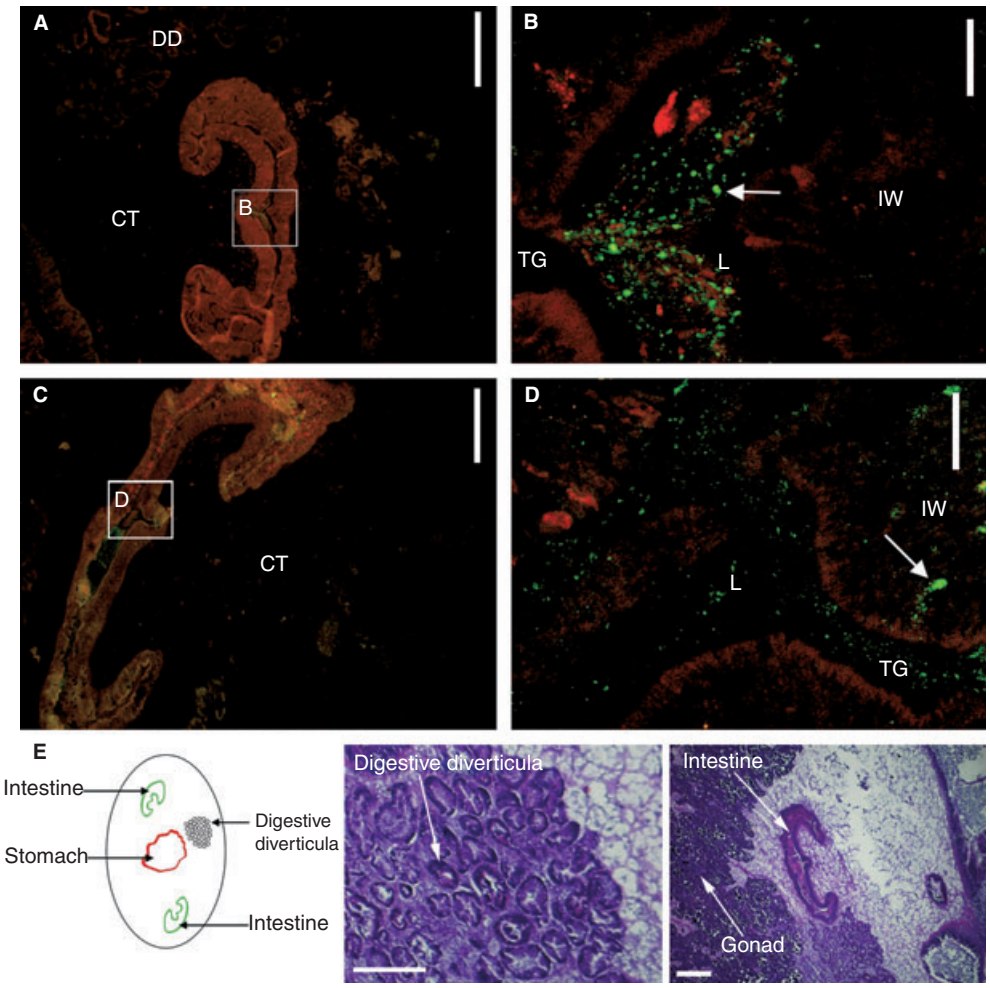

Figure 4 Localization of PV and NoV IR in the intestine (midgut). PV and NoV IR (green) were visualized with an AlexaFluor 488 conjugated secondary antibody, and cell nuclei and cytoplasm were counterstained with propridium iodide (red). Panel A shows a low power view of the intestine. Panel B shows an enlargement of the boxed region of Panel A in which PV IR can be seen in the lumen of the intestine (arrow). Panel C shows staining for NoV IR in an equivalent section to that presented in Panel A. Panel D shows an enlarged portion of Panel C and the arrow points to NoV IR inside the intestine wall. Panel E shows a schematic representation of a cross-section through a oyster, along with Haemalun and Eosin-stained sections of digestive diverticula and intestine. CT = connective tissue; TG = typhlosole groove; L = intestine lumen; IW = intestine wall; DD = digestive diverticula. Scale bars on Panels A and C = 200 μm. Scale bars on Panels B and D = 20 μm.

B. Little NoV IR was observed in the intestine lumen among food particles and mucus (Panel D) but NoV IR was observed within the intestine epithelium (Panel D, white arrow). Staining in the intestine epithelium was sparse and irregular in comparison with IR observed in the stomach epithelium.

Digestive diverticula and connective tissue

We also observed PV and NoV IR in the lumen of the digestive diverticula and inside small round structured cells within the digestive diverticula epithelium. Figure 5A shows PV IR (green) in the lumen of a digestive diverticula tubule (white arrow). Panels B–D show NoV IR detected by DAB staining. Black arrows in Panels B and C show NoV IR inside small round cells in the connective tissue (CT) and digestive diverticula epithelium, respectively. IR in the digestive diverticula tubules was variable with some tubules showing staining in the lumen, others in the epithelium, and yet others were devoid of IR. Panel D shows NoV IR in the same small round cells identified in Panels B and C, but in the connective tissue surrounding the stomach.

Labial palps and gills

Figure 6A presents a low power view of oyster labial palp folds (PF) counterstained with propridium iodide. PV IR (green) can be seen on the distal sides of PF. The labial PF lean forward slightly in the direction of the mouth

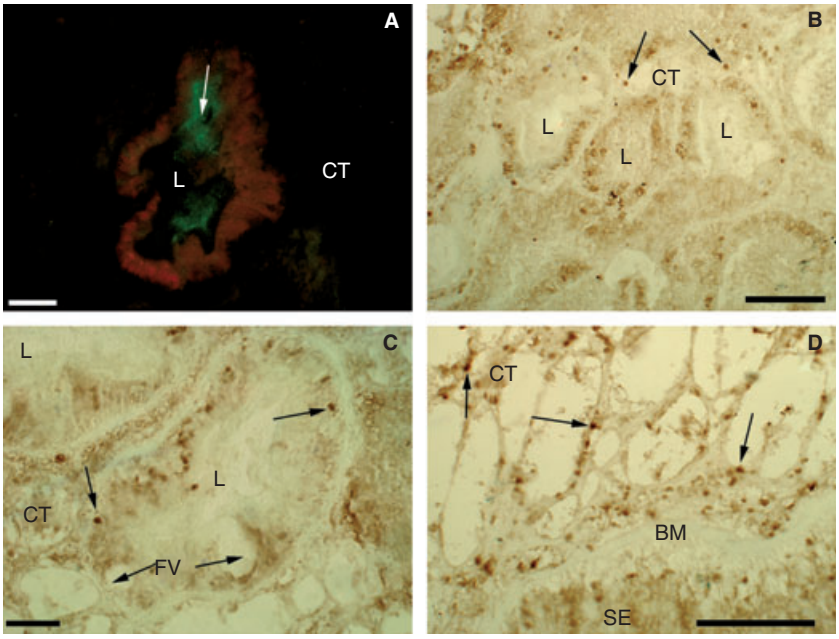

Figure 5 Localization of PV and NoV IR in the digestive diverticula. PV IR (Panel A) was detected as in Fig. 3, and NoV IR by DAB staining (dark brown, Panels B–D). Panel A shows PV IR inside the lumen of a digestive diverticula tubule (arrow). Panels B–D shows NoV IR inside small round cells located within connective tissue surrounding the digestive diverticula tubules, the digestive diverticula epithelium and within the connective tissue surrounding the oyster stomach, respectively (arrows). L = lumen; FV = food vacuole; CT = connective tissue; SE = stomach epithelium; BM = basement membrane. Scale bars panels A and C = 20 μm. Scale bars panels B and D = 50 μm.

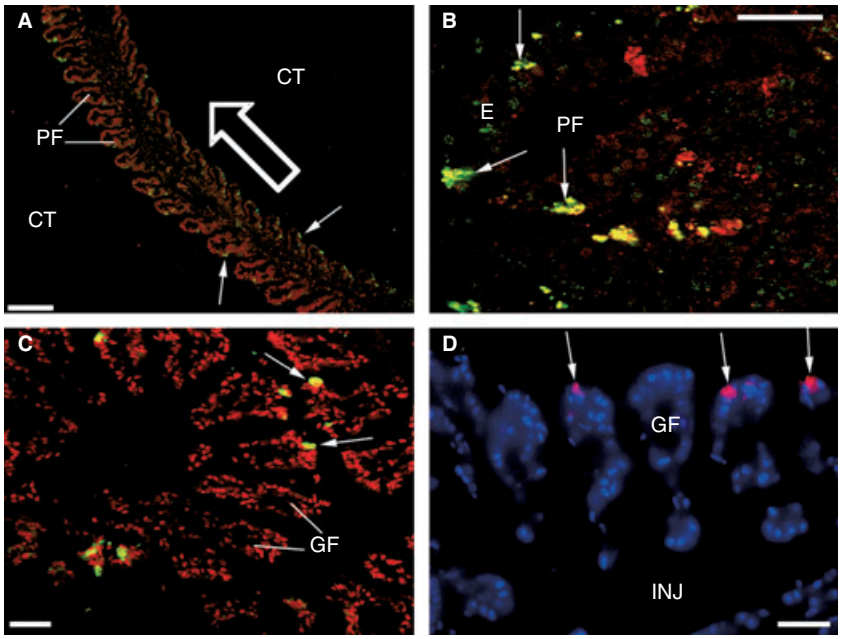

Figure 6 Localization of PV IR in the gill and labial palp. PV IR was visualized using a secondary antibody conjugated withier either AlexaFluor 488 (green, Panels A–C) or Rhodamine (red, Panel D). Cell nuclei and cytoplasm are counterstained with either propridium iodide (red Panels A–C) or DAPI (blue, Panel D). Panel A shows PV immunoreactivity (IR; white arrows) on the distal sides of the palp folds. The direction of flow towards the mouth is indicated by the large arrow. Panel B shows PV IR present inside the labial palp epithelium (arrows). Panels C and D show PV IR on and within the gill epithelium (arrows). CT = connective tissue; PF = palp fold; GF = gill filament; E = palp epithelium; INJ = interfilamentar junction. Scale bar Panel A = 200 μm. Scale bars Panels B–D = 20 μm.

and PV IR is predominantly localized on the distal side of the PF that faces away from the oyster mouth (Fig. 6A, white arrows). The direction of water flow, towards the mouth, is indicated by a large arrow. Panel B is a higher magnification image showing PV IR both within and on the epithelium of the labial PF (white arrows). PV staining is also detected cyoplasmically within the labial palp epithelium (Panel B, white arrows), as was found for the epithelium of the digestive tract. PV IR in other regions of the labial PF was sparse. NoV IR was not observed in sections of the labial PF.

Figure 6, Panels C and D show PV IR within and on the gill epithelium similar to that observed for the labial PF; staining for PV was localized to either the surface of the gill, or cytoplasmically within the gill epithelium. Figure 6C shows PV IR (green) on the tips of the gill filaments (white arrows, counterstained red), consistent with the virus adhering to the exterior of the gill filament.

Panel D shows PV IR localized to the cytoplasm of the gill filament epithelium.

Discussion

Tissue distribution and localization of PV and NoV in Pacific oysters

We show that PV and NoV RNA are present in the digestive tract, gill and labial palp tissues of oysters that have been feeding in virus-contaminated water. Fewer viruses were present in the labial palp and gill tissue, compared with the digestive tract tissue, as determined by real-time RT-PCR. Consistent with this both PV and NoV IR was observed in the lumen and epithelium of the digestive tract tissue (including the stomach, intestine and digestive diverticula), and in nondigestive tract tissue (connective tissue). While PV IR was observed in the labial palps and gills NoV was not, which was consistent with the relatively low NoV PCR results for these tissues. This is mostly likely a consequence of the lower level of NoV in the inoculum used and lower sensitivity of IHC compared with RT-PCR; however, the potential occurrence of NoV IR in the labial palps and gills of more heavily contaminated oysters cannot be precluded. Indeed, other IHC experiments undertaken in our laboratory indicate the presence of NoV IR in oyster gill sections (Seamer 2007).

The pattern of IHC staining within tissues of the digestive tract that we observed is similar to that reported by others using different *in situ* techniques. Romalde *et al.* (1994) used *in situ* transcription and autoradiography to localize HAV in digestive tract tissues of the eastern oyster (*Crassostrea virginica*) and reported the presence of HAV in the basal cells of the ciliated epithelium of the stomach, and in the digestive diverticula. Our findings are also consistent with that of Le Guyader *et al.* (2006) who used IHC techniques to show the presence of NoV in the lumen of the digestive diverticula, and in phagocytes between the epithelial cells of the digestive diverticula, after 12 and 24 h bioaccumulation by Pacific oysters. Similarly, Hay and Scotti (1986) used radiolabeled cricket paralysis virus (CrPV) to demonstrate that virus was in cells of the digestive diverticula and mid-gut epithelium of Pacific oysters.

Literature regarding the *in situ* distribution of human enteric viruses in oyster cells that are outside of the digestive tract is scarce. In this study, we identified PV IR both on and within the epithelial cells of the labial PF. The localization of PV to the distal side of the labial palps is most likely related to the flow of mucus and virus across the distal palp surface. However, we were able to detect NoV IR in the connective tissue consistent with the findings of Le Guyader *et al.* (2006) who also have reported NoV in the connective tissue of oysters. Similarly, our report of PV IR in the gills of infected oysters is consistent with other studies that have used cell culture techniques to identify PV in experimentally infected oysters (Di Girolamo *et al.* 1975). Dore and Lees (1995) also used cell culture to investigate tissue distribution of F+ bacteriophage in mussels (*Mytilus edulis*) and found that small amounts of F+ bacteriophage were detected in the labial palps and gills.

Although of similar size and morphology (i.e. spherical, icosahedral symmetry), functionally significant differences in the capsid proteins of the viruses used in this study result in differences in surface properties and receptor binding (Greenberg *et al.* 1981; Glass *et al.* 2000; Hardy 2005). The results of ours and other studies; however, indicate that the distribution and localization of bioaccumulated virus in Pacific oyster tissues is similar for a number of different virus types.

Phagocytes and virus uptake

Phagocytes are reported to be abundant in various oyster tissues including between the stomach epithelial cells, in the connective tissue surrounding the digestive tract, in the intestine lumen, between epithelial cells in the digestive diverticula, between gill epithelial cells and on the surface of the gill, and between labial palp epithelial cells (Yonge 1926; Barnes 1980). The location of oyster phagocytes reported in the literature coincides with the location of virus protein observed by IHC in this study. In addition, IR was observed in our study in cells of many different shapes (e.g. small round cells and thin elongated cells), consistent with the highly variant shape of phagocytes (Tripp *et al.* 1966). Other *in vivo* and *in vitro* studies have also suggested that phagocytes take up virus particles (Fries and Tripp 1970; Fisher 1986; Le Guyader *et al.* 2006). Whilst the IHC results we report and that of other studies are consistent with the internalization of viruses by phagocytes, further studies are required to elucidate and definitively confirm the cell type(s) responsible for virus uptake.

Virus content of seawater

Data from a variety of shellfish-growing waters over a 7-year period in the United States indicated average levels of 0·2 viruses ml^{-1} seawater (Metcalf 1982). Levels in New Zealand waters are probably lower than this, in the order of 1×10^{-5} to 1×10^{-3} viruses ml^{-1} seawater (G. Lewis, University of Auckland, NZL, personal communication). In order to facilitate the detection of viruses much higher levels of virus than that encountered in shellfish-growing waters were used in these bioaccumulation experiments (80 NoV PAU ml^{-1} and 37 500 PV PAU ml^{-1}). It would

be useful in future studies to further explore the kinetics of virus uptake by Pacific oysters when varying amounts of virus are present in the overlaying seawater.

Conclusion

The results of this study confirm the presence of human enteric viruses within cells of digestive tract and nondigestive tract oyster tissues. The relative amount of virus in the nondigestive tissues is small; however, it has been suggested that very low numbers of enteric viruses are capable of inducing illness in humans (Caul 1994; Moe *et al.* 1999; Moe 2001). Thus, even low numbers of infective viruses present in nondigestive tract tissues of oysters pose a risk to human health. From the data, we have presented, outbreaks of illness that have followed consumption of depurated bivalves may be attributed to the presence of viruses in cells outside the digestive tract. Viruses present in the oyster digestive tract lumen are probably removed relatively rapidly via defecation when oysters are placed in clean water; however, elimination or inactivation of virus that has been taken into oyster cells may take a longer period of time, as such, consumption of depurated bivalves still poses a potential health risk. In addition, many methods of analysis fail to identify the presence of viruses in tissues outside the digestive tract because of the limitations in sensitivity of detection methods, and the common utilization of methods that test only digestive tract tissues. It is recommended that when assessing the efficacy of depuration or relaying to remove viruses from oysters that the presence of viruses within cells and in tissues outside the digestive tract is taken into consideration, and that the absence of viruses within the digestive tract not be taken as an indication of the absence of viruses within the bivalve *per se*.

Acknowledgements

This work was funded by the Public Good Science Fund of New Zealand Ministry of Science, Research and Technology, Contracts C03X0301 and C03X0204. FRhK-4 cells were kindly provided by Dr M.D. Sobsey (University of North Carolina, Chapel Hill, USA). An ESR Postgraduate Scholarship supported CM. The authors especially thank Jim Dollimore of Biomarine Limited for provision of oysters, and the New Zealand Food Safety Authority for additional funding.

References

Ashida, M. and Hamada, C. (1997) Molecular cloning of the hepatitis A virus receptor from a simian cell line. *J Gen Virol* **78**, 1565–1569.

Atmar, R.L., Metcalf, T.G., Neill, F.H. and Estes, M.K. (1993) Detection of enteric viruses in oysters by using the polymerase chain reaction. *Appl Environ Microbiol* **59**, 631–635.

Barnes, R. (1980) *Invertebrate Zoology*, 4th edn ed. Barnes, R. Philadelphia: Saunders College.

Bendinelli, M. and Ruschi, A. (1969) Isolation of human enterovirus from mussels. *J Appl Microbiol* **18**, 531–532.

Büchen-Osmond, C. (2004) The Universal Virus Database, version 3: ICTVdB Management Internet source: http://www.ncbi.nlm.nih.gov/ICTVdb/ICTVdB/. Downloaded November 2006. New York, USA: Columbia University.

Butt, A.A., Aldridge, K.E. and Sanders, C.V. (2004) Infections related to the ingestion of seafood Part I: Viral and bacterial infections. *Lancet Infect Dis* **4**, 201–212.

Caul, E.O. (1994) Small round structured viruses: airborne transmission and hospital control. *Lancet* **343**, 1240–1242.

Chironna, M., Germinario, C., De-Medici, D., Di-Pasquale, S., Quarto, M. and Barbuti, S. (2002) Detection of hepatitis A virus in mussels from different sources marketed in Puglia (Southern Italy). *Int J Food Microbiol* **75**, 12–18.

Di Girolamo, R., Liston, J. and Matches, J. (1975) Uptake and elimination of poliovirus by west coast oysters. *J Appl Microbiol* **29**, 260–264.

Donaldson, K.A., Griffin, D.W. and Paul, J.H. (2002) Detection, quantitation and identification of enteroviruses from surface waters and sponge tissue from the Florida Keys using real-time RT-PCR. *Water Res* **36**, 2505–2514.

Dore, W.J. and Lees, D.N. (1995) Behaviour of *Escherichia coli* and male-specific bacteriophage in environmentally contaminated bivalve molluscs before and after depuration. *Appl Environ Microbiol* **61**, 2830–2834.

Feigelstock, D., Thompson, P., Mattoo, P., Zhang, Y. and Kaplan, G.G. (1998) The human homolog of HAVcr-1 codes for a hepatitis A virus cellular receptor. *J Virol* **72**, 6621–6628.

Fisher, W. (1986) Structure and functions of oyster hemocytes. In *Immunity in Invertebrates* ed. Brehelin, M. pp. 25–35. Berlin: Springer.

Formiga-Cruz, M., Tofino-Quesada, G., Bofill-Mas, S., Lees, D.N., Henshilwood, K., Allard, A.K., Conden-Hansson, A.C., Hernroth, B.E. *et al.* (2002) Distribution of human virus contamination in shellfish from different growing areas in Greece, Spain, Sweden, and the United Kingdom. *Appl Environ Microbiol* **68**, 5990–5998.

Fries, C.R. and Tripp, M.R. (1970) Uptake of viral particles by oyster leukocytes *in vitro*. *J Invertebr Pathol* **15**, 136–137.

Glass, P.J., White, L.J., Ball, J.M., Leparc-Goffart, I., Hardy, M.E. and Estes, M.K. (2000) Norwalk virus open reading frame 3 encodes a minor structural protein. *J Virol* **74**, 6581–6591.

Green, D. and Lewis, G.D. (1999) Comparative detection of enteric viruses in wastewaters, sediments and oysters by reverse transcription-PCR and cell culture. *Water Res* **33**, 1195–1200.

Greenberg, H.B., Valdesuso, J.R., Kalica, A.R., Wyatt, R.G., McAuliffe, V.J., Kapikian, A.Z. and Chanock, R.M. (1981) Proteins of Norwalk virus. *J Virol* **37**, 994–999.

Greening, G., Mirams, M. and Berke, T. (2001a) Molecular epidemiology of 'Norwalk-like viruses' associated with gastroenteritis outbreaks in New Zealand. *J Med Virol* **64**, 58–66.

Greening, G.E., Dawson, J. and Lewis, G. (2001b) Survival of poliovirus in New Zealand green-lipped mussels, *Perna canaliculus*, on refrigerated and frozen storage. *J Food Prot* **64**, 881–884.

Hardy, M.E. (2005) Norovirus protein structure and function. *FEMS Microbiol Lett* **253**, 1–8.

Hay, B. and Scotti, P. (1986) Evidence for intracellular absorption of virus by the Pacific oyster, *Crassostrea gigas*. *N Z J Mar Freshwater Res* **20**, 655–659.

Hewitt, J. and Greening, G.E. (2004) Survival and persistence of norovirus, hepatitis A virus, and feline calicivirus in marinated mussels. *J Food Prot* **67**, 1743–1750.

Hollinger, F.B. and Emerson, S.U. (2001) Hepatitis A Virus. In *Fields Virology* eds. Knipe, D.M. and Howley, P.M. pp. 799–840. Philadelphia: Lippincott-Raven Publishers.

Howard, D.W. and Smith, C.S. (1983) *Histological Techniques for Marine Bivalve Mollusks*. National Marine Fisheries Serivce, Woods Hole, MA No. NOAA-TM-NMFS-F/NEC-25. Springfield: Northeast Fisheries Center.

Jones, N. and Graham, J. (1995) Outbreak of gastroenteritis associated with oysters: a Norwalk-like virus most likely cause. *N Z Public Health Rep* **2**, 25–26.

Kapikian, A.Z., Estes, M.K. and Chanock, R.M. (1996) Norwalk group of viruses. In *Fields Virology* eds. Fields, B.N., Knipe, D.M. and Howley, P.M. pp. 783–810. Philadelphia: Lippincott-Raven Publishers.

Kivell, B.M., Day, D.J., McDonald, F.J. and Miller, J.H. (2004) Developmental expression of mu and delta opioid receptors in the rat brainstem: evidence for a postnatal switch in micro isoform expression. *Brain Res Dev Brain Res* **148**, 185–196.

Koopmans, M., von Bonsdorff, C.H., Vinje, J., de Medici, D. and Monroe, S. (2002) Foodborne viruses. *FEMS Microbiol Rev* **26**, 187–205.

Le Guyader, F., Loisy, F., Atmar, R.L., Hutson, A.M., Estes, M.K., Ruvoen, N., Pommepuy, M. and Le Pendu, J. (2006) Norwalk virus-specific binding to oyster digestive tissues. *Emerg Infect Dis* **12**, 931–936.

Lees, D. (2000) Viruses and bivalve shellfish. *Int J Food Microbiol* **59**, 81–116.

Lewis, G., Loutit, M. and Austin, F. (1986) Enteroviruses in mussels and marine sediments and depuration of naturally accumulated viruses by green lipped mussels (*Perna canaliculus*). *N Z J Mar Freshwater Res* **20**, 431–437.

Lowther, J.A., Henshilwood, K. and Lees, D.N. (2008) Determination of norovirus contamination of oysters from two commercial harvesting areas over an extended period, using semiquantitative real-time reverse transcription PCR. *J Food Prot* **71**, 1427–1433.

Metcalf, T.G. (1982) Viruses in shellfish-growing waters. *Environ Int* **7**, 21–27.

Moe, C. (2001) Studies of the infectivity of Norwalk and Norwalk-like viruses – *summary of research project* Internet source downloaded November 2006. http://es.epa.gov/ncer/science/drinkingwater/moe_r826139.pdf. Chapel Hill: University of North Carolina.

Moe, C., Sobsey, M., Stewart, P. and Crawford-Brown, D. (1999) Estimating the risk of human calicivirus infection from drinking water. Abstract. In *International Workshop on Human Caliciviruses*. Atlanta, USA.

Racaniello, V.R. (2001) Picornaviridae: the viruses and their replication. In *Fields Virology* eds. Fields, B.N., Knipe, D.M. and Howley, P.M. pp. 685–722. Philadelphia: Lippincott-Raven Publishers.

Racaniello, V.R. (2006) One hundred years of poliovirus pathogenesis. *Virology* **344**, 9–16.

Romalde, J.L., Estes, M.K., Szucs, G., Atmar, R.L., Woodley, C.M. and Metcalf, T.G. (1994) *In situ* detection of hepatitis A virus in cell cultures and shellfish tissues. *Appl Environ Microbiol* **60**, 1921–1926.

Schwab, K.J., Neill, F.H., Estes, M.K., Metcalf, T.G. and Atmar, R.L. (1998) Distribution of Norwalk virus within shellfish following bioaccumulation and subsequent depuration by detection using RT-PCR. *J Food Prot* **61**, 1674–1680.

Seamer, C. (2007). The biology of virus uptake and elimination by Pacific oysters (*Crassostrea gigas*). PhD Thesis, Victoria University of Wellington, Wellington, New Zealand.

Shumway, S., Cucci, T., Newell, R. and Yentsch, C.M. (1985) Particle selection, ingestion and absorption in filter-feeding bivalves. *J Exp Biol Ecol* **91**, 77–92.

Simmons, G., Greening, G., Gao, W. and Campbell, D. (2001) Raw oyster consumption and outbreaks of viral gastroenteritis in New Zealand: evidence for risk to the public's health. *Aust N Z J Public Health* **25**, 234–240.

Tripp, M.R., Bisignani, L.A. and Kenny, M.T. (1966) Oyster amoebocytes *in vitro*. *J Invertebr Pathol* **8**, 137–140.

Ward, J., Levinton, J., Shumway, S. and Cucci, T. (1997) Site of particle selection in a bivalve mollusc. *Nature* **390**, 131–132.

Ward, J., Levinton, J., Shumway, S. and Cucci, T. (1998) Particle sorting in bivalves: *in vivo* determination of the pallial organs of selection. *Mar Biol* **131**, 283–292.

Wong, M.L. and Medrano, J.F. (2005) Real-time PCR for mRNA quantitation. *Biotechniques* **39**, 75–85.

Yonge, C. (1926) Structure and physiology of organs of feeding and digestion in *O. edulis*. *J Mar Biol Assoc UK* **14**, 295–386.

Zheng, D.P., Ando, T., Fankhauser, R.L., Beard, R.S., Glass, R.I. and Monroe, S.S. (2006) Norovirus classification and proposed strain nomenclature. *Virology* **346**, 312–323.

